Optimization of Stranded-Wire Windings and Comparison with Litz Wire on the Basis of Cost and Loss

Xu Tang
C. R. Sullivan

Found in *IEEE Power Electronics Specialists Conference,* June 2004, pp. 854–860.

Optimization of Stranded-Wire Windings and Comparison with Litz Wire on the Basis of Cost and Loss.

Xu Tang and Charles R. Sullivan
Email: charles.r.sullivan@dartmouth.edu http://engineering.dartmouth.edu/inductor
8000 Cummings Hall, Dartmouth College, Hanover, NH 03755, USA

***Abstract*— Stranded wire with uninsulated strands has been proposed as a low-cost alternative to litz wire. In this paper, we develop a method to optimize stranded-wire designs on the basis of cost and loss, and compare the results to optimized litz-wire designs. A simply calculated parameter is shown to be useful to predict when each type of wire is preferred. A method to extend both loss prediction and optimization for arbitrary geometries and waveforms is also introduced.**

Deliberate oxidation of strands is proposed as a method to improve performance of stranded wire, and to increase its range of applicability. Experimental measurements with approximately 0.15 μm oxide show dramatic increases in interstrand resistivity, indicating that this approach could be very effective.

I. Introduction

Simple stranded wire without insulation on the individual strands has recently been proposed as a cost-effective substitute for litz wire for reducing eddy-current loss in high-frequency transformer and inductor windings [1]. Although it seems self-evident that the individual copper strands that constitute litz wire should be insulated to prevent circulating currents and to effect the function of litz wire in reducing losses, stranded wire with uninsulated strands, which we will refer to simply as *stranded wire*, can be expected to reduce circulating currents significantly compared to solid wire. It provides an intermediate alternative between the extremes of litz wire and solid wire on both cost and the potential to reduce circulating currents.

It appears that stranded wire is a useful alternative to consider where the high cost of litz wire is prohibitive and slightly higher losses can be tolerated. However, in such a situation, it is also possible to choose a lower cost litz-wire design. Choosing a litz-wire design is difficult, because of the large design space of possible choices for number and diameter of strands, many of which have high cost, high loss, or both. Hence, careful optimization can be invaluable; the methods in [2], [3], [4] narrow the design space to a smaller set of alternatives, each of which provides the lowest possible loss at any given cost. Thus, in order to determine when and where stranded wire offers advantages, it is necessary to compare a range of optimized designs, and show that the stranded wire can provide lower cost at a given loss, or lower loss at a given cost. We undertake such a comparison in this paper, by combining the loss analysis of stranded wire in [1] with the optimization of litz wire in [2].

Previous work on loss calculation in stranded wire is reviewed in Section I-A. A method to find the lowest-loss stranded-wire design for any given cost is described in Section IV, based on a cost model developed in Section II. Section III discusses an important parameter in the model: interstrand resistivity, and introduces and tests a method to improve it. The loss model is used to compare optimized stranded- and litz-wire designs in Section V, including finding a simple calculation that can be applied to a given design problem to determine whether stranded wire will be advantageous. In Section VI, the methods of Sections I-A, IV and V are extended to address arbitrary waveforms that may be different in each winding and two-dimensional (2-D) and three-dimensional (3-D) field geometries.

This work was supported in part by the United States Department of Energy under grant DE-FC36-01GO1106.

A. Loss Calculation

The calculation of high-frequency effects in stranded wire developed in [1] is reviewed briefly here, and in more detail in Appendix I.

High-frequency winding loss effects include skin effect (the tendency for high-frequency currents to flow on the surface of a conductor) and proximity effect (the tendency for current to flow in other undesirable patterns—loops or concentrated distributions—due to the presence of magnetic fields generated by nearby conductors). Ordinarily, proximity-effect losses are dominant over skin-effect losses because in a multi-layer winding the total magnetic field is much larger than the field generated only by one strand or turn. For this reason, the loss calculation in [1] focuses on proximity-effect loss.

In multi-strand windings, proximity-effect loss includes effects at both the strand level and the bundle level, as illustrated in Fig. 1. Strand-level proximity effect may optionally be still further divided into internal proximity effect (the effect of other currents within the bundle) and external proximity effect, but we instead consider the total proximity effect as a result of the total field at any given strand [2]. Strand-level effects are usually not affected by the presence or absence of insulation and standard litz-wire analysis [5], [6], [7], [8] can be applied to uninsulated strands. The effect of increased length due to twisting is addressed in [1], as reviewed in Appendix I, resulting in this expression for power loss due to strand-level proximity effect:

$$P_{\text{eddy, strand}} = \frac{\pi\omega^2\overline{\hat{B}^2}d_s^4 n\ell}{128\rho_c}\left(1+\frac{\pi^2 n d_s^2}{4K_a p^2}\right) \qquad (1)$$

where ω is the radian frequency of the sinusoidal excitation, ℓ is the length of the bundle, ρ_c is the resistivity of copper, p is the pitch of the twisting, n is the number of strands in a bundle, d_s is the diameter of each strand, $\overline{\hat{B}^2}$ is the spatial

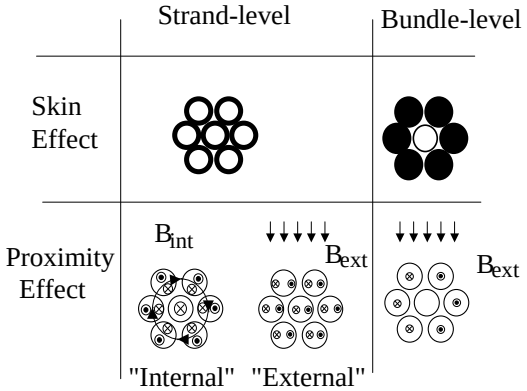

Fig. 1. Types of eddy-current effects in bundled wire.

average of the squared peak magnetic flux density, and K_a is the strand packing factor, which is assumed to be independent of the pitch. This model (1) is only valid if the strand diameter is smaller than or comparable to a skin depth [9], [10], as is the case in good litz- or stranded-wire designs. For 1-D field geometries, the average squared field can be easily calculated [11], [10]. An approach for more complicated geometries and for non-sinusoidal waveforms is discussed in Section VI.

Predicting bundle-level proximity effect with finite conductivity between strands is more complex than predicting strand-level effects. For this calculation, the conductivity between strands is characterized by an effective resistivity of the composite material comprising many strands, ρ_{ss}, measured perpendicular to the strand or bundle axis. Typical values of ρ_{ss} range from 20 $\mu\Omega$·m to 200 $\mu\Omega$·m [1]. This important parameter is discussed in more detail in Section III.

As reviewed in Appendix I, [1] derives an expression for the bundle-level proximity-effect loss.

$$P_{\text{eddy, bundle}} = \frac{p^2\omega^2\overline{\hat{B}^2}nd_s^2\ell}{32\rho_{ss}\pi K_a}(1+\frac{n\pi^2 d_s^2}{4K_a p^2}). \qquad (2)$$

This expression has been experimentally verified in [1].

From (2), we see that the bundle-level eddy-current loss decreases as pitch is reduced. However, the other losses, $P_r = I_{rms}^2 R_{dc}$ and the strand-level eddy-current loss $P_{\text{eddy, strand}}$ given by (1), increase as pitch is reduced. Thus, the total loss has a minimum value at an intermediate, optimal pitch, p_{opt}. In [1], this optimal pitch is found to be

$$p_{opt} = \sqrt[4]{\frac{\pi^4\rho_{ss}nd_s^4}{16\rho_c} + \frac{32I_{rms}^2\rho_{ss}\pi^2\rho_c}{\omega^2\overline{\hat{B}^2}nd_s^2}} \qquad (3)$$

where I_{rms} is the rms current in the winding under consideration.

II. Cost Modelling

As discussed in [8], [2], optimizing litz-wire designs without considering cost leads to the use of very large numbers of fine strands that are prohibitively expensive. Thus, practical optimization must include a cost model, particularly given that the goal of using stranded wire is to reduce cost.

As was done in [2] for litz wire, we developed a curve-fit function for the cost per unit mass of stranded wire from manufacturers' pricing.

$$C_{m,\text{copper}}(d_s) = 0.46 + \frac{0.49\times10^{-26}\,\text{m}^6}{d_s^6} + \frac{2.5\times10^{-9}\,\text{m}^2}{d_s^2} \qquad (4)$$

The cost $C_{m,\text{copper}}(d_s)$ in (4) is for stranded copper wire with no strand insulation or bundle insulation, and is normalized to a value of one for the cost per unit mass of large-strand litz wire, so that the values can be compared directly with costs from the curve-fit model for litz-wire cost in [2],

$$C_{m,\text{litz}}(d_s) = 1 + \frac{1.1\times10^{-26}\,\text{m}^6}{d_s^6} + \frac{2\times10^{-9}\,\text{m}^2}{d_s^2} \qquad (5)$$

which has the same normalization.

For stranded wire, there is an additional complication: It is necessary to insulate the overall bundle before a winding can be constructed, whereas with litz wire, it is possible to rely only on the strand insulation, or to add only serving (a textile wrap) to mechanically protect the strands while still relying on the strand insulation for electrical isolation between turns. A thermoplastic insulation, such as PTFE (Teflon), PVC, polyester, polyuretahne, or polypropylene can be extruded over a litz- or stranded-wire winding. The relative cost and temperature ratings of these materials are listed in Table I. The cost of this insulation is an important factor in determining whether and when stranded wire is competitive with litz wire.

In some applications, thermoplastic such as PTFE is used for bundle insulation on litz wire in order to increase the dielectric strength for high voltage or for safety requirements. In such cases, stranded wire is significantly cheaper. However, in other litz applications where no bundle insulation is used, the extra cost of the bundle insulation must be subtracted from the cost savings of using stranded wire.

We have also developed an approximate model for the cost of coating per unit length, again based on manufacturers' pricing:

$$C_{\text{coating}} = k_{c1}\sqrt{\frac{n}{K_a}}d_s + k_{c2} \qquad (6)$$

Coating litz wire costs more than coating stranded wire because litz wire is more suceptible to mechanical and thermal damage. Thus, the constant k_{c1} takes on different values for coating litz or stranded wire with the same PTFE insulation ($2\times10^{-5}\,\text{m}^{-1}$ or $1.5\times10^{-5}\,\text{m}^{-1}$, respectively). For PTFE insulation, the same value for k_{c2} is used for either case, 2.4×10^{-9}. With these constants, (6) gives normalized values compatible with (4) and (5). (i.e., as in (4) and (5), the values are normalized to a value of one for large-strand litz wire.)

TABLE I
Relative cost and operation temperature of several bundle insulation materials.

	Polypropylene	PVC	Polyester	Polyurethane	PTFE
Relative cost	1	1.25	4	5	7
Operation temperature ^{o}C	80	105	180	180	200

This means that (4), (5), and (6) can be used together to compare costs of different strategies. Note that the constants in these formulas are subject to change as wire technology changes. However, even with different constants, the structure of the model and general conclusions are likely to remain unchanged.

III. Interstrand Resistivity

The interstrand resistivity could, in theory, be larger than the bulk resistivity of copper because of two different effects. Firstly, current flowing between strands must crowd into a narrow contact area. This "bottleneck" introduces extra resistance. However, extensive analysis of this effect, including calculations of contact area as a function of pressure and finite-element analysis of the current flow [12], showed that the resistance produced by this effect is much smaller than values measured in practice, using measurement methods described in [1]. Thus, we conclude that the resistance must be mostly produced by contact resistance and surface contamination, for example by a thin layer of surface oxidation.

Because even slight oxidation seems to substantially enhance resistance between strands, we propose increasing resistivity by deliberately introducing slight oxidation. The oxidation of copper is a complex process. The oxidation rate depends on several factors including the temperature and gas composition [13]. Different forms of oxidation rate laws are observed in different temperature ranges [13]. At high temperatures (above 800^o C), a parabolic rate law is observed [13]:

$$\frac{d\xi}{dt} = \frac{k_1}{\xi} \tag{7}$$

where ξ is the thickness of oxidation layer, t is the oxidation time and k_1 is the parabolic scaling constant. At intermediate temperatures (200 to 800^o C), a cubic law is observed [13]:

$$\frac{d\xi}{dt} = \frac{k_2}{\xi^2} \tag{8}$$

At lower temperatures (lower than 200^o C), the oxidation rate follows a reciprocal logarithmic law [13]. We can save time by oxidizing the strands at very high temperature (above 1000^o C). For simplicity in testing, we choose to oxidize the strands at intermediate temperatures. For our purposes, we do not need to find a mathematical model for oxidation in the temperature range we are interested in, but can instead directly find the thickness of oxidation layer grown in a given time at a specific temperature from experimental data. Ten minutes of oxidation at 256^o C in normal air gives an oxidation layer of thickness 0.15 μm as calculated in [12] from the experimental data in [13]. The oxidation thickness is much smaller than the strand diameter (the diameter of strand 40 AWG is about 80 μm, and the thickness of a single-build magnet wire insulation is about 8 μm). The increase of DC resistance of a strand by such an oxidation layer can be ignored.

In order to detect the loss difference between bare and oxidized stranded wire, we need to choose wire in which the bundle-level proximity-effect loss dominates over the strand-level proximity-effect loss. Comparing (1) with (2), we find large pitch and small strand diameter should be used to achieve this goal. So we chose wire consisting of 210 strands of 40 AWG with a pitch of 30 mm. We oxidized the strands of one sample for 10 minutes at 200^o C in normal air in an oven and then twisted the oxidized strands into a bundle. The oven was pre-warmed to 200^o C before strands were put into it. We used the direct proximity-effect loss measurement method described in [1] to measure the proximity-effect loss in both clean and oxidized wire samples, and found the interstrand resistivity by fitting the predicted curve to the measured curve. Note that the strand-level proximity loss is not affected by interstrand resistivity.

For the bare stranded wire, an interstrand resistivity of 150 $\mu\Omega$·m is chosen to fit the measured curve, while for the oxidized stranded wire, an interstrand resistivity of 450 $\mu\Omega$·m is chosen to fit the measured curve. The interstrand resistivity is increased by about a factor of three due to oxidation. And this resistivity is about 25 times the worst-case number of 20 $\mu\Omega$·m for bare wire [1]. In these two wire samples, the bundle-level loss dominates over strand-level loss. The total loss in the wire is reduced by about a factor of three due to the oxidation of strands. We also find that oxidized stranded wire is easier to solder than litz wire.

In the wire industry, the typical annealing temperature is about 700^o C. At this temperature, the oxidation rate is about 100 times faster than at 200^o C. This means an oxidation layer of thickness 0.15 μm can be grown in less than 10 seconds. Thus oxidation of strands is a practical way to improve the performance of stranded wire.

IV. Optimization

There are many possible combinations of strand diameter and number of strands (d_s and n) for any given cost. We wish to find the combination that, for a given cost, provides the minimum loss. For a particular strand size, d_s, we can calculate the number of strands, n, for the given cost, and then calculate the power loss using the loss model described in Section I-A. Thus, for a fixed cost, we can calculate the loss for any given strand diameter. We then use a numerical optimization routine (the Nelder-Mead Simplex algorithm [14] as implemented in the MATLAB function `fminsearch`) to find the strand diameter that yields the minimum power loss for the given cost. We repeat this procedure for different costs to find the minimum loss for any given cost. A flowchart of this process is shown in Fig. 2.

V. Comparing Litz and Stranded Wire

One way to compare litz wire and stranded wire is through an example. We start by considering the same design example used in [2] (RM5 ferrite core, number of turns $N = 14$, frequency $f = 1$ MHz, bobbin window breadth $b_b = 4.93$ mm, core window breadth $b_c = 6.3$ mm). Curves of minimum loss at any given cost are shown for PTFE coated litz-wire and PTFE stranded-wire windings with and without strand oxidation in Fig. 3.

At the upper left of Fig. 3, the cost of the stranded-wire winding is lower than the cost of the litz-wire winding for

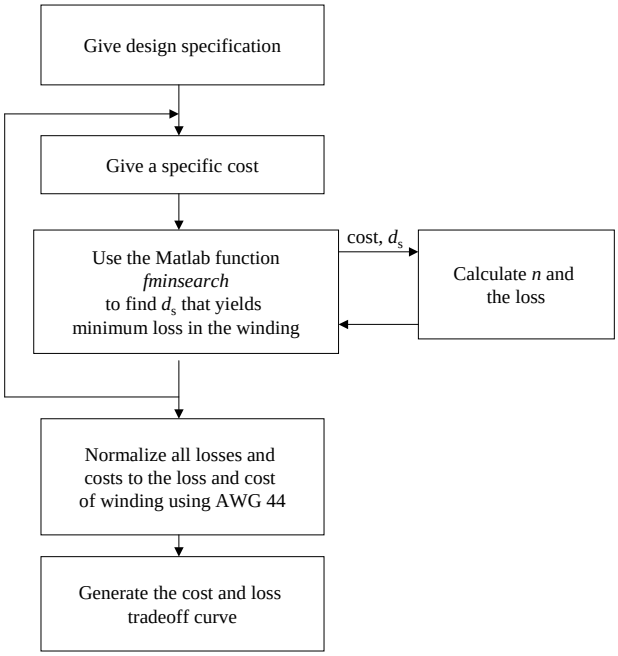

Fig. 2. Flowchart of the procedure to generate cost and loss tradeoff curves.

the same loss. However, for a given increase in cost (corresponding to using finer strands), the loss reduction is greater for litz wire than for stranded wire. There is a point at which the two curves intersect and to the right of this point, the litz-wire winding performs better than the stranded-wire winding. We denote the intersection point as the critical strand diameter, d_{crit}. If we have a design using a litz-wire winding with strand diameter larger than d_{crit}, a stranded-wire winding can provide the same performance at a lower cost, whereas for designs using strand diameters smaller than d_{crit}, stranded wire offers no advantage. Note that the oxidation significantly extends the region in which stranded wire has an advantage.

Although Fig. 3 clearly shows the cost and loss ranges

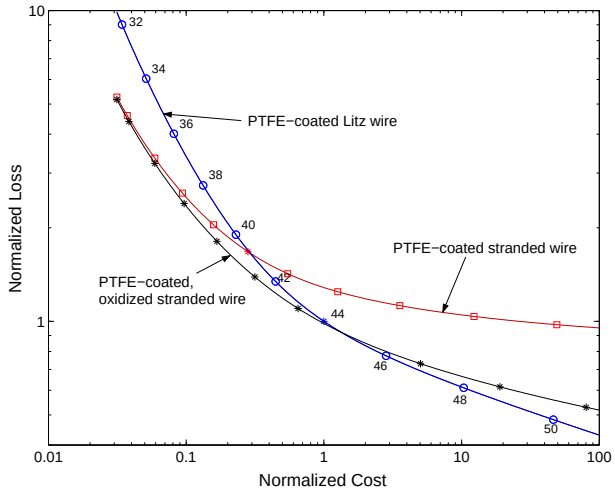

Fig. 3. Cost and loss, for PTFE-coated litz-wire and PTFE-coated stranded-wire windings, with and without oxidation. All are normalized to an optimal cost/loss design using a PTFE-coated litz-wire winding with 44 AWG strands.

in which litz- or stranded-wire windings are preferable, the designer must still make a choice between lower-loss, higher-cost designs and higher-loss, lower-cost designs. Given detailed information on the application, one can calculate the cost of the power losses over the life of the equipment, and compare that to the cost of a lower-loss winding as described in [2]. However, it may be desirable to use lower loss designs than this simple calculation alone would indicate, because there may be additional equipment and energy-cost savings from reduced cooling requirements, and because of the environmental benefits of reduced energy consumption.

Returning to the question of whether to choose litz or stranded wire, we find that the position of the point at which the two curves intersect changes with six different parameters. It would be desirable to find a parameter that is a combination of all these parameters such that the curve only depends on the one new parameter. We suppose this parameter has the following form:

$$X = b_c \rho_c^{a_1} N^{a_2} f^{a_3} \rho_{ss}^{a_4} K_a^{a_5} \tag{9}$$

Through a series of numerical experiments, we found X to be

$$X = \frac{b_c \sqrt{\rho_c}}{N f \rho_{ss} K_a^2} \tag{10}$$

As long as this parameter stays constant, the intersection point does not change (d_{crit} stays constant). Fig. 4 shows d_{crit} changing with X. A simple calculation of X provides an easy way for a designer to determine whether stranded wire is advantageous in a particular design, without the effort of performing the full optimization of either type of winding. After calculating X from (10) and finding d_{crit} from Fig. 4, a designer knows the range of strand diameters in which stranded wire is advantageous. Note that Fig. 4 applies regardless of whether oxidation is used; oxidation factors into the value of X such that the same curve applies, but a given design now falls on a different point on the curve. The larger the value of X, the smaller the range of strand sizes for which stranded wire is preferred. So if we have a design with a small value of X, which corresponds to large number of turns, high operation frequency and relatively small core window width, stranded wire is often advantageous.

The comparison between litz and stranded wire depends on whether one is considering using thermoplastic insulation on both, or on only the stranded wire, and it depends on the type of thermoplastic used. In our cost models and in the price quotes we have seen, PTFE insulated stranded wire is always more expensive than litz wire without bundle insulation. Thus, litz wire is always preferred in that comparison. However, stranded wire is often preferred if PTFE bundle insulation would be used on the litz wire anyway. If PVC or other less expensive bundle insulation can be used on the stranded wire, stranded wire may be lower in cost even if no bundle insulation is needed on the litz wire. Table II compares these costs, and Fig. 4 includes a curve for this comparison (PVC insulation on the stranded wire and no bundle insulation on the litz wire) as well as a curve for PTFE on both types of wire. Both curves indicate a substantial range in which stranded wire is advantageous. The same example plotted in Fig. 3 is analyzed

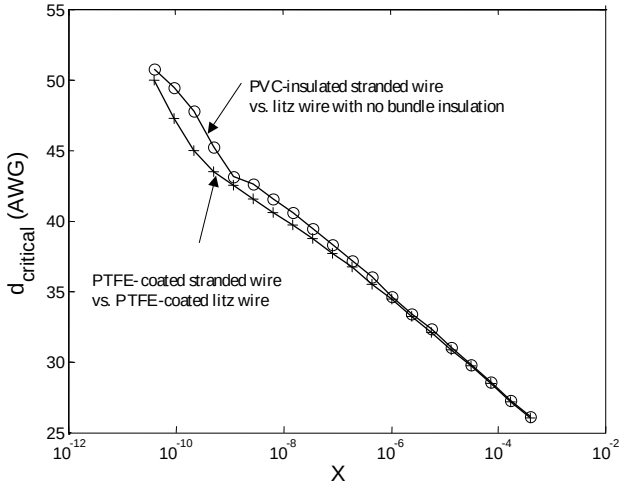

Fig. 4. Critical strand diameter as a function of X. For a given design, X can be calculated, and d_{crit} can be found from this curve. The best design choices are then stranded wire with strand diameter larger than d_{crit} or litz wire with strand diameter smaller than d_{crit}. Two curves are shown: one for the choice between litz wire and stranded wire, both with PTFE bundle insulation; and one for the choice between litz wire without bundle insulation and stranded wire with PVC insulation.

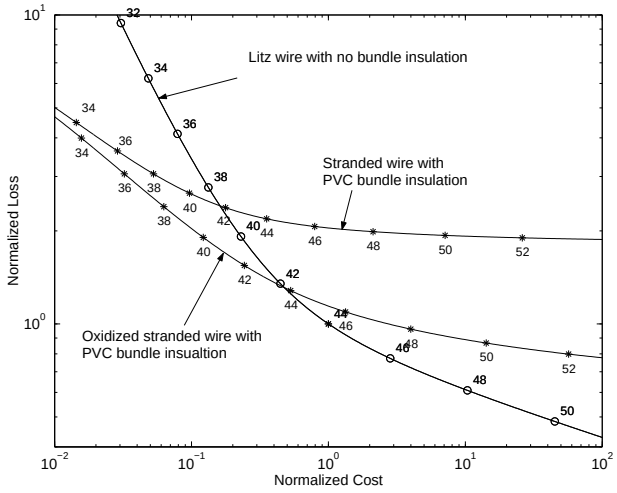

Fig. 5. Tradeoff lines for stranded wire with PVC bundle insulation and litz wire with no bundle insulation. Also a tradeoff line for oxidized stranded wire with PVC bundle insulation is shown. An interstrand resistivity $\rho_{ss} = 450\ \mu\Omega$·m is used for oxidized stranded wire.

TABLE II

RELATIVE COST PER UNIT LENGTH OF LITZ WIRE WITH NO BUNDLE INSULATION AND STRANDED WIRE WITH PVC BUNDLE INSULATION.

	32	36	40	44	50
Litz wire with no bundle insulation	6.82	2.86	1.36	1	4.76
Stranded wire with PVC bundle insulation	4.57	2.11	1.46	1.01	3.03

All wires consist of 105 strands. Costs are normalized to a value of one for litz wire using 44 AWG strands.

again in Fig. 5, but this time comparing stranded wire with PVC insulation to litz wire with no insulation, rather than PTFE insulation on both. Note that although the regions where stranded wire shows an advantage are similar in Figs. 3 and 5, the size of the advantage is bigger in Fig. 5.

VI. MODIFICATION OF LOSS MODEL FOR ARBITRARY WAVEFORMS AND 2-D OR 3-D FIELD GEOMETRY

Our loss-prediction model is developed based on sinusoidal waveforms and 1-D field analysis. This section modifies the loss model for arbitrary waveforms and 2-D or 3-D field geometry, based on the squared field derivative (SFD) method for calculating loss [15], which is reviewed in Appendix II.

The ac resistance factor, $F_r = R_{ac}/R_{dc}$, for a litz-wire winding with sinusoidal waveforms and 1-D field geometry [5], [6], [7], [8] can be expressed:

$$F_r = 1 + \frac{\pi^2\omega^2\mu_0^2 N^2 n^2 d_s^2}{768\rho_c^2 b_c^2} = 1 + k_\ell n_j^2 A_{s,j}^2 \qquad (11)$$

where b_c is the breadth of the core window, N is the number of turns, k_ℓ represents constant terms in the first form of the expression lumped together, A_s is the cross-sectional area of a strand and the subscript j indicates the jth winding in a multi-winding transformer. In [3], a procedure for calculating k_ℓ for arbitrary waveforms and 2-D or 3-D field geometry is derived, such that (11) can still be used to accurately calculate losses, including the effects of fringing fields, mutual resistance effects [16], and non-sinusoidal waveforms. The calculation of k_ℓ [3] is based on the squared field derivative (SFD) method for calculating loss [15]; the necessary formulas are summarized in Appendix II-A.

If we can rewrite the stranded-wire loss model in terms of k_ℓ, we will be able to use the method in [3] (Appendix II-A) to calculate k_ℓ and it will possible to calculate loss in stranded wire for arbitrary waveforms and 2-D or 3-D field geometries. The ac resistance factor, F_r, for a stranded-wire winding can be expressed as:

$$F_r = 1 + \frac{P_{\text{eddy, strand}}}{P_r} + \frac{P_{\text{eddy, bundle}}}{P_r} \qquad (12)$$

where P_r is resistive power loss, $I_{rms}^2 R_{dc}$. We insert the expression for optimal pitch (3) into the equation for $P_{\text{eddy, bundle}}$ (2) and find F_r as a function of k_ℓ:

$$F_r = 1 + k_\ell n^2 A_s^2 \left(1 + \frac{A_s}{K_a}\sqrt{\frac{\rho_c}{\rho_{ss}}}\sqrt{n + \frac{1}{k_\ell n A_s^3}}\right) \qquad (13)$$

Thus for any given core geometry and arbitrary waveforms, we can calculate the value of k_ℓ using the method provided in Appendix II-A (from [3]) and then find the power loss in a stranded-wire winding from:

$$P = F_r P_r = F_r \frac{I_{rms}^2 \ell}{n A_s} \qquad (14)$$

where F_r is calculated from (13). In addition to using this approach to calculate power loss, we can use the method described in Section IV to generate cost and loss tradeoff curves. The curves of critical diameter based on the parameter X can also be used for arbitrary waveforms and geometries if we calculate X in terms of k_ℓ by comparing an expression for X with an expression for k_ℓ, both based on the simple 1-D

sinusoidal case. The result is:

$$X = \frac{\mu_0}{\rho_{ss} K_a^2} \sqrt{\frac{\pi}{2\rho_c} \frac{1}{k_\ell}}. \quad (15)$$

This allows one to determine whether a design with arbitrary waveforms and geometries is a good candidate for stranded wire by using the curves in Fig. 4; the applicability of the analysis based on X is no longer limited to simple geometries and waveforms.

VII. Conclusion

Stranded wire is an attractive low-cost alternative to litz wire, but only in certain situations. Because of the large design space of number and diameter of strands, and because of the possibility of incurring very high loss if these parameters are not chosen carefully, it is important to truly optimize either a litz- or stranded-wire design. We have introduced a method to optimize stranded-wire designs based on the experimentally verified loss analysis in [1]. A simply calculated parameter has been introduced to predict when each type of wire is preferred. A method to extend both loss prediction and optimization for arbitrary geometries and waveforms has also been introduced.

Deliberate oxidation of strands is proposed as a method to improve performance of stranded wire, and to increase its range of applicability. Experimental measurements with approximately 0.15 μm oxide show dramatic increases in interstrand resistivity, indicating that this approach could be very effective.

Appendix I
Loss Calculation in Stranded Wire

The loss calculations in [1] are briefly reviewed below. Because the bundle-level proximity effect losses are reduced by using smaller pitch, it is important to include the effect of pitch on dc resistance and on strand-level proximity effect.

A. DC resistance

The distance a strand travels is longer when it is twisted than when it goes straight. With simple twisting, each strand will stay within one cylindrical shell at a radius r, and thus will be longer than the overall bundle by a factor of

$$\frac{\ell_d}{p} = \frac{1}{\cos(\theta)} = \frac{\sqrt{p^2 + (2\pi r)^2}}{p} \quad (16)$$

where p is the pitch, θ is the angle relative to straight axial travel, and ℓ_d is the actual length of the strand.

The overall dc resistance of a twisted bundle is the parallel combination of the resistances of many such strands, each at a different radius. Because of the different resistances, the dc current will not be exactly equal for each strand. However, calculations are simplified by assuming that the dc current flowing in each strand is the same, and this approximation was shown in [1] to be good to better than 2% when the pitch is more than six times the diameter of the bundle. On this basis, the dc resistance is found in [1] to be

$$R_{dc} = \frac{4\rho_c \ell}{\pi n d_s^2} \left(1 + \frac{\pi^2 n d_s^2}{4 K_a p^2}\right) \quad (17)$$

where ℓ is the length of the bundle, ρ_c is the resistivity of copper, and K_a is a strand-packing factor defined in [1] as

$$K_a = \frac{A_e}{A_b} \quad (18)$$

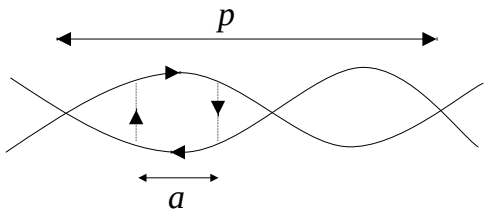

Fig. 6. Integration loop used to find voltage that induces current flow along the marked path.

where A_b is the overall bundle area and A_e is the sum of the cross sectional areas of all the strands, with the strand areas taken perpendicular to the bundle, not perpendicular to the strands, such that the cross sections are elliptical.

In (17), the factor $\frac{4\rho_c \ell}{\pi n d_s^2}$ represents resistance without twisting, and the expression in the parentheses represents the effect of pitch.

B. Strand-level eddy-current loss

Standard proximity-effect power loss models [5], [7], [8], [17] for fine strands (assuming the strand to be small compared to a skin depth at the frequency of interest [9], [10], which will the case for good designs) can be modified to include the effect of twisting as for dc resistance, resulting in

$$P_{\text{eddy, strand}} = \frac{\pi \omega^2 \overline{\hat{B}^2} d_s^4 n \ell}{128 \rho_c} \left(1 + \frac{\pi^2 n d_s^2}{4 K_a p^2}\right) \quad (19)$$

where $\overline{\hat{B}^2}$ is the spatial average of the square of the peak value of the ac flux density, $\hat{B}$, and $B(t)$ varies at a radian frequency ω.

In typical transformer designs, a standard 1-D model of the field is sufficient to obtain the average value of $\hat{B}^2$ [11], [10],

$$\overline{\hat{B}^2} = \frac{1}{3} \cdot \left(\frac{\mu_0 N \hat{I}}{b_w}\right)^2 \quad (20)$$

where b_w is the width of the winding window, N is the number of turns and $\hat{I}$ is the peak current.

C. Bundle-level eddy-current loss

In a twisted bundle with significant resistance between strands, the potential between a pair of strands can be calculated as the derivative of the integral of the flux linked by the path shown in Fig. 6. The area of the loop in Fig. 6 varies with the distance a between the positions where potential is evaluated. We assume that the flux is uniform throughout the bundle; that the eddy currents are not large enough to significantly reduce the flux. The situation in which eddy current is large enough to reduce the flux is discussed in [1].

In a given cross section through the bundle, different strands are at different points in the twist cycle, corresponding to different values of a. Thus, the potential difference between a strand and the strand in the corresponding position on the opposite side of the bundle may be calculated as a function of the position in the bundle. This potential drives the currents between strands. Reference [1] approximates the network of discrete resistances between strands as a continuous medium described by a resistivity ρ_{ss} in the plane perpendicular to the axis. Thus, current and loss can be calculated from the electric field which is found from the gradient of potential. The resulting time-average bundle-level proximity-effect loss is calculated in [1] to be

$$P_{\text{eddy, bundle}} = \frac{p^2 \omega^2 \overline{\hat{B}^2} n d_s^2 \ell}{32 \rho_{ss} \pi K_a} \left(1 + \frac{n \pi^2 d_s^2}{4 K_a p^2}\right). \quad (21)$$

APPENDIX II
THE SFD METHOD FOR LOSS CALCULATION WITH ARBITRARY WAVEFORMS AND GEOMETRIES

The SFD method [15] is a generalized version of an approach to nonsinusoidal waveforms that has been widely used [8], [18], [19], [20]. It is based on the dependence of losses on the squared derivative of the field, $(\frac{dB}{dt})^2$. It is valid when the diameter of a strand is small compared to a skin depth, as is the case for a well-designed litz-wire or stranded-wire winding.

Given the dependence of loss on $(\frac{dB}{dt})^2$, and given that B is a linear function of the current in different windings, it is possible to account for the losses resulting from these different currents using a "dynamic loss matrix" $\mathbf{D}$ [15]

$$P_{eddy} = \overline{\left[\begin{array}{cc} \frac{di_1}{dt} & \frac{di_2}{dt} \end{array}\right] \mathbf{D} \left[\begin{array}{c} \frac{di_1}{dt} \\ \frac{di_2}{dt} \end{array}\right]}. \quad (22)$$

The matrix $\mathbf{D}$ is calculated, independent of current waveforms, using a series of simplified magnetostatic field simulations—one for each winding excited alone, and one for each possible pair of windings. The accuracy of the SFD method has been experimentally verified in [15].

A. Evaluation of k_ℓ

The approach in Section VI is based on lumping factors that may arise from conventional analysis or from the SFD method into a factor k_ℓ, such that the optimization approaches developed for simple waveforms and geometries apply more generally. This approach was developed in [3].

To most easily find k_ℓ for a particular winding ($k_{\ell,j}$), [3] defines a modified dynamic resistance matrix with the stranding parameters n and A_s factored out: $\tilde{\mathbf{D}} = \frac{\mathbf{D}}{n_j A_{s,j}^2}$, and uses only the portion of $\tilde{\mathbf{D}}$ associated with losses in the winding of interest: $\tilde{\mathbf{D}}_\mathbf{j}$. Reference [15] calculates $\mathbf{D}$ in terms of a loss coefficient, γ_j for each winding j, which accounts for the influence of the stranding parameters on $\mathbf{D}$. To remove that influence, [3] defines a modified loss coefficient:

$$\tilde{\gamma}_j = \frac{\gamma_j}{n_j A_{s,j}^2} = \frac{\ell_{w,j}}{4\pi\rho_c}. \quad (23)$$

Here, ℓ_w is the length of the entire winding, equal to the average length of a turn multiplied by the number of turns: $\ell_w N \ell_t$.

One can calculate $\tilde{\mathbf{D}}_j$ from $\tilde{\gamma}_j$ and from the results of magnetostatic field calculations of the field due to unit current in each winding [3]. The calculation of $\tilde{\mathbf{D}}$ is expressed in terms of the field due to unit current in winding m, $\hat{\vec{B}}_m$, as

$$\tilde{\mathbf{D}}_j = \tilde{\gamma}_j < \left[\begin{array}{cc} \left|\hat{\vec{B}}_1\right|^2 & \hat{\vec{B}}_1 \cdot \hat{\vec{B}}_2 \\ \hat{\vec{B}}_2 \cdot \hat{\vec{B}}_1 & \left|\hat{\vec{B}}_2\right|^2 \end{array}\right] >_j \quad (24)$$

where $<>_j$ signifies the spatial average over the region of the winding j. As derived in [3], these parameters can be used to express k_ℓ as

$$k_{\ell,j} = \frac{\overline{\left[\begin{array}{cc} \frac{di_1}{dt} & \frac{di_2}{dt} \end{array}\right] \tilde{\mathbf{D}}_j \left[\begin{array}{c} \frac{di_1}{dt} \\ \frac{di_2}{dt} \end{array}\right]}}{I_{rms,j}^2 \ell_{w,j} \rho_c}. \quad (25)$$

ACKNOWLEDGMENT

Thanks to New England Wire Technologies Corp., Lisbon, NH, USA, for producing special wire samples.

REFERENCES

[1] X. Tang and C. R. Sullivan, "Stranded wire with uninsulated strands as a low-cost alternative to litz wire," in *IEEE Power Electronics Specialists Conference*, 2003.

[2] C. R. Sullivan, "Cost-constrained selection of strand wire and number in a litz-wire transformer winding," *IEEE Transactions on Power Electronics*, vol. 16, no. 2, Mar. 2001.

[3] C. Sullivan, T. Abdallah, and T. Fujiwara, "Optimization of a flyback transformer winding considering two-dimensional field effects, cost and loss," in *Proceedings of 16th Annual Applied Power Electronics Conference - APEC 2001*, 2001, pp. 116–22 vol.1.

[4] J. Pollock, T. Abdallah, and C. R. Sullivan, "Easy-to-use CAD tools for litz-wire winding optimization," in *IEEE Applied Power Electronics Conference*, 2003.

[5] P. N. Murgatroyd, "Calculation of proximity losses in multistranded conductor bunches," *IEE Proceedings, Part A*, vol. 36, no. 3, pp. 115–120, 1989.

[6] J. A. Ferreira, "Analytical computation of ac resistance of round and rectangular litz wire windings," *IEE Proceedings-B Electric Power Applications*, vol. 139, no. 1, pp. 21–25, Jan. 1992.

[7] B. B. Austin, "The effective resistance of inductance coils at radio frequency," *The Wireless Engineer*, vol. 11, pp. 12–16, Jan. 1934, summary of work by S. Butterworth.

[8] C. R. Sullivan, "Optimal choice for number of strands in a litz-wire transformer winding," *IEEE Transactions on Power Electronics*, vol. 14, no. 2, pp. 283–291, 1999.

[9] X. Nan and C. R. Sullivan, "An improved calculation of proximity-effect loss in high-frequency windings of round conductors," in *34th Annual IEEE Power Electronics Specialists Conference*, 2003.

[10] ——, "Simplified high-accuracy calculation of eddy-current loss in round-wire windings," in *35th Annual IEEE Power Electronics Specialists Conference*, 2004.

[11] R. W. Erickson and D. Maksimovic, *Fundamentals of Power Electronics*, 2nd ed. Kluwer Academic Publishers, 2001.

[12] X. Tang, "Stranded wire with uninsulated strands as a low-cost alternative to litz wire," Master's thesis, Dartmouth College, 2003.

[13] K. Hauffe, *Oxidation of Metals*. Plenum Press, 1965.

[14] J. Lagarias, J. Reeds, M. Wright, and P. Wright, "Convergence properties of the Nelder-Mead simplex method in low dimensions," *SIAM Journal on Optimization*, vol. 9, no. 1, pp. 112–47, 1998.

[15] C. R. Sullivan, "Computationally efficient winding loss calculation with multiple windings, arbitrary waveforms, and two- or three-dimensional field geometry," *IEEE Transactions on Power Electronics*, vol. 16, no. 1, 2001.

[16] J. H. Spreen, "Electrical terminal representation of conductor loss in transformers," *IEEE Transactions on Power Electronics*, vol. 5, no. 4, pp. 424–9, 1990.

[17] E. C. Snelling, *Soft Ferrites, Properties and Applications*, 2nd ed. Butterworths, 1988.

[18] S. Crepaz, "Eddy-current losses in rectifier transformers," *IEEE Transactions on Power Apparatus and Systems*, vol. PAS-89, no. 7, pp. 1651–1662, 1970.

[19] P. N. Murgatroyd, "The torroidal cage coil," *IEE Proceedings, Part B*, vol. 127, no. 4, pp. 207–214, 1980.

[20] W. Hurley, E. Gath, and J. Breslin, "Optimizing the ac resistance of multilayer transformer windings with arbitrary current waveforms," *IEEE Transactions on Power Electronics*, vol. 15, no. 2, pp. 369–76, Mar. 2000.